J. Biochem. **144,** 457–466 (2008)
doi:10.1093/jb/mvn088

The Unfolding of α-Momorcharin Proceeds Through the Compact Folded Intermediate

Yukihiro Fukunaga, Etsuko Nishimoto, Takuhiro Otosu, Yasutaka Murakami and Shoji Yamashita*

Institute of Biophysics, Faculty of Agriculture, Kyushu University, Hakozaki, Higashi-ku, Fukuoka 812-8581, Japan

Received April 9, 2008; accepted July 1, 2008; published online July 4, 2008

The unfolding of α-momorcharin was systematically investigated using steady-state and time-resolved tryptophan fluorescence, circular dichroism and 8-anilino-1-naphthalenesulfonic acid (ANS) binding. These spectroscopic studies demonstrated that α-momorcharin unfolded through a compact folded intermediate state. The content of α-helix was increased, Trp192 approached closer to the side of active site and its rotational motion was restricted by being equilibrated with 2–3 M of guanidine hydrochloride. Furthermore, the binding of ANS with α-momorcharin was more suppressed to show that the hydrophobic parts would not be accessed to the protein surface but rather be sealed off in this specific conformation state. These results suggest that the structure of α-momorcharin holds the more compact conformation as an incipient state for unfolding, which is the sharp contrast to β-momorcharin that gives the characteristics of the generally known molten globule state.

Key words: α-momorcharin, fluorescence energy transfer, molten globule, protein folding/unfolding, time-resolved fluorescence depolarization.

Abbreviations: ANS, 8-anilino-1-naphthalenesulfonic acid; CD, circular dichroism; Gdn, guanidine hydrochloride; MG, molten globule; RIPs, ribosome-inactivating proteins; TCSPC, time-correlated single photon counting.

Momorcharin is one of the ribosome-inactivating proteins (RIPs) and works as the bio-defense relating protein since it catalyses the adenine-releasing reaction from ribosomal RNA to prohibit the protein synthesis. Now, two types of momorcharin, α- and β-momorcharin were found and they are isolated from seeds of bitter gourd. Their X-ray crystallographic structures and sequences of amino acids have been already confirmed. These two types of momorcharins retain high similarity in structure and homology in the sequence of amino acid each other. The active site of the momorcharin is composed of arginine, glutamate and two tyrosine residues. As shown in Fig. 1, a single tryptophan residue is arranged adjacently to the active site to cover up the lid for the active site (*1*). Because of such specific arrangement of the tryptophan residue and active site, momorcharin is a quite interesting subject for studying the protein folding/unfolding process and mechanism through the fluorescence spectroscopy. It is considered that the active site of the enzyme uniquely maintains the more compact conformation in the protein to complete the specific biological roles. Besides, the tryptophan residue works as an excellent reporter for the subtle conformational change induced in the protein. Generally, the tryptophyl fluorescence has been used as a convenient tool for monitoring the protein folding/unfolding process and kinetics using its specific photophysical properties depending on the polarity of the surrounding circumstances. Furthermore, the tryptophan residue in protein is more useful if the more advanced techniques such as time-resolving fluorescence spectroscopic methods are applied. The information on the interaction between the peptide elements and the dynamics of the conformational fluctuation can be uniquely obtained by the fluorescence decay analysis of the tryptophan residue specified its location in protein (*2*). These are indispensable entities for characterizing the feature of the conformation of proteins. Furthermore, the spectroscopic methods based on the resonance excitation energy transfer formulation and the analysis of the time-resolved fluorescence depolarization would be also expected to be useful to figure out the unique conformation and dynamics of the folding/unfolding intermediate of proteins.

Recently, we reported the features of the unfolding intermediate state of β-momorcharin formed in the equilibratory denaturing condition (*3*). The hydrophobic domains of β-momorcharin were exposed to the protein surface and the motional freedom of tryptophan residue was increased without loosing the secondary structure at the intermediate state. These properties of the partially unfolded state almost coincide with the general concepts of molten globule (MG) state. In the present studies, we characterized the unfolding intermediate state of α-momorcharin using the time-resolved fluorescence spectroscopy and the results were compared with the intermediate state of β-momorcharin previously characterized.

*To whom correspondence should be addressed. Tel/Fax: +81-92-642-4425, E-mail: yamashita@brs.kyushu-u.ac.jp

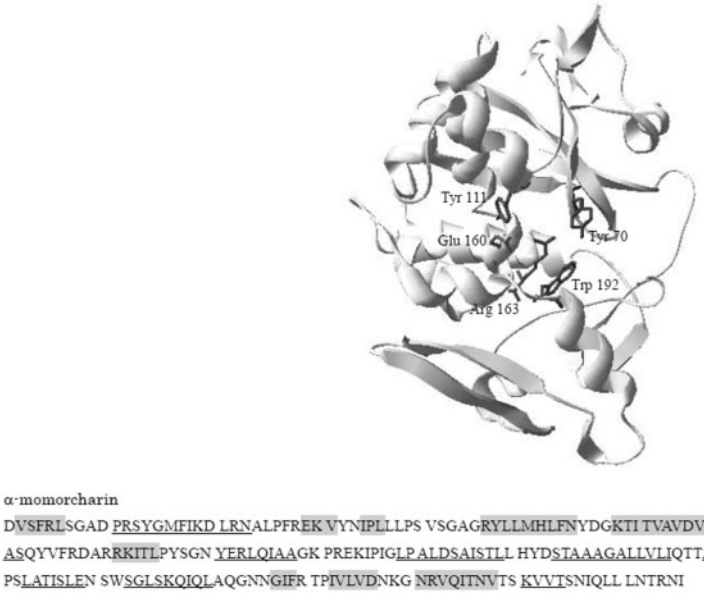

Fig. 1. **Structure of α-momorcharin.** The side chains of the amino acid residues constituting the active site and Trp192 are shown. The figure is based on PDB file, 1CF5 (*12*).

The MG state of protein is considered to be the general folding/unfolding intermediate state of proteins. The systematic studies on MG state are desirable to elucidate the protein folding mechanism because the essential factors that mediate between the native and unfolded state would be densely inscribed in the structural, physical and chemical features of MG state. The conformation and thermodynamic properties of MG state have been investigated using various biophysical techniques and the fundamental properties have been well defined (*4–11*). However, our knowledge has not reached to the level to understand the folding mechanism and to predict accurately the final structure. In the trial to elucidate the protein folding mechanism, one key factor is the amino acid sequence of protein. Anfinsen proposed that three dimensional structure of protein is predominantly determined by the amino acid sequence (*12*, *13*). Based on his dogma, it is not unreasonable to consider that the proteins with higher homology in the sequence and high similarity in the native structure may exhibit the similar equilibrium folding/unfolding profile and properties in the MG state each other. But this assumption is not necessarily hold as seen in the case of the relation between lysozyme and α-lactalbumin (*14*). These two proteins are very homologous in amino acid sequence and 3D structure. But, α-lactalbumin adopts the typical MG state in the equilibrium state with the mild concentration of the chemical denaturant or high acidic condition. On the other hand, the distinctive MG state of lysozyme has not been recognized yet. As seen in this case, more detailed information on the fundamental properties such as the site specific interaction and packing of peptide elements in the intermediate state of the proteins with similar sequences should be cleared to elucidate the protein folding/unfolding mechanism, stability and eventually, the protein function. The comparative studies on the folding/unfolding intermediate states of α-momorcharin and β-momorcharin are very interesting, because they have similar 3D structures and amino acid sequences. In the present study, the characteristic properties exhibited in the unfolding intermediate state of α-momorcharin were investigated using the fluorescence spectroscopic methods.

MATERIALS AND METHODS

Materials—Seeds of bitter gourd (*Momordica charantia*) were purchased from Nakahara Co. Ltd. (Fukuoka, Japan) Guanidine hydrochloride (Gdn), 8-anilino-1-naphthalenesulfonic acid (ANS) and other chemicals were of highest grade and used without further purification. Mono-S and DEAE-Sepharose used for the ion-exchange chromatography were purchased from GE Healthcare Bio-Science Corp. (Buckinghamshire, UK)

Purification and Preparation of α-Momorcharin—The purification of α-momorcharin was performed according to the methods of Fong *et al*. (*15*). The trashed seeds of bitter gourd were ground and homogenized in 2 mM sodium phosphate buffer, pH 7.5. The resulting slurry was stirred for 5 h to extract the crude proteins. After removing the insoluble components by filtration and centrifugation at 30,000*g* for 1 h at 4°C, the crude protein solution was dialysed against 2 mM sodium phosphate buffer, pH 7.5. The dialysed sample was applied to DEAE-Sepharose column equilibrated with the same buffer. The unbound proteins were applied to Mono-S column equilibrated with 2 mM sodium phosphate buffer, pH 7.5, and eluted by linear gradient of 0–0.5 M of NaCl. The fraction corresponding to α-momorcharin, which was confirmed by the *N*-glycosidase activity against RNA was concentrated and dialysed against 20 mM Tris–HCl buffer, pH 7.8. Every chromatography was performed on BioLogic DuoFlow system (BioRad, Hercules, CA) at 4°C. The purity of α-momorcharin was examined by

SDS–PAGE and the gel-filtration chromatography on HPLC.

The purified α-momorcharin was dissolved in 20 mM of Tris–HCl buffer, pH 7.8 for the equilibratory unfolding experiments. Small aliquot of the stock sample solution was added to the reaction mixture containing the desired concentration of Gdn. This protein solution was incubated at 25°C for 6 h to reach the equilibrium. In these conditions, no further changes in any spectroscopic properties of α-momorcharin were recognized after the incubation. The concentration of α-momorcharin was determined spectrophotometrically using $OD_{280} = 1.3$ (1 mg/ml).

Steady-state and Time-resolved Fluorescence Measurements—The steady-state fluorescence emission spectra were recorded on Hitachi 850 fluorescence spectrophotometer. The fluorescence emission spectrum was strictly corrected against the detection and excitation systems. The undesired effects of stray lights were also removed with a subtraction method. The fluorescence spectrum of ANS was measured for the protein solution including 20 μM of α-momorcharin, which was equilibrated with various concentrations of Gdn. The excitation wavelengths, 297 and 380 nm were used for α-momorcharin and ANS, respectively. The steady-state fluorescence anisotropy of α-momorcharin was measured with the same instrumentation. Based on the definition, the fluorescence anisotropy (r) was calculated after the measurements of the vertical (I_{vv}) and horizontal (I_{vh}) fluorescence intensities against the vertical excitation. The G-factor is determined by the ratio of I_{hv} to I_{hh}, which were the intensities vertically and horizontally polarized components against the horizontal excitation, respectively.

The time-resolved fluorescence and fluorescence anisotropy were measured with the sub-picosecond laser-based time-correlated single photon counting method (TCSPC). The excitation pulse (275–300 nm) was separated from a combination of sub-picosecond Ti:sapphire laser (Tsunami, Spectra-Physics, Stratford, CT), pulse picker with second harmonic generator (model 3980, Spectra-Physics) and third harmonic generator (GWU, Spectra-Physics). The repetition rate was 800 kHz and the obtained excitation pulse width was 100 fs. The stop pulse to drive the time-to-amplitude converter (TAC, 457, Ortec, Oak Ridge, TN) was detected by a high speed APD (C5658, Hamamatsu Photonics, Shizuoka, Japan). The fluorescence emission pulse was detected a multi-channel plate type photomultiplier (3809U-50, Hamamatsu Photonics) and fed into TAC through a constant fraction discriminator (935, Ortec). The output signals of TAC were accumulated in 2,048 channels in multi-channel analyser (Maestro-32, Ortec). The channel width was 11 ps/ch.

The fluorescence decay kinetics of α-momorcharin was described with linear combination of some exponentials,

$$F(t) = \sum \alpha_i \exp\left(\frac{-t}{\tau_i}\right) \quad (1)$$

where, τ_i is the fluorescence decay time of i-th component and α_i is the corresponding pre-exponential factor, α_i and τ_i were determined with the iterative convolution and non-linear curve-fitting methods. The adequacy of the curve fitting was judged by the residual plots and statistic parameters such as serial variance ratio (SVR) and sigma value (σ) (*16*).

The measurements of the fluorescence anisotropy decay were performed with the same TCSPC system. But, a Gran–Taylor polarizer was set at the just behind the sample to measure the decays of vertical [$I_{vv}(t)$] and horizontal [$I_{vh}(t)$] components against the vertical excitation. $I_{vv}(t)$ and $I_{vh}(t)$ were related with the fluorescence decay, $F(t)$ and anisotropy decay, $r(t)$ by the following Eqs 2 and 3.

$$I_{vv}(t) = \frac{1}{3}F(t)\{1 + 2r(t)\} \quad (2)$$

$$I_{vh}(t) = \frac{1}{3}F(t)\{1 - r(t)\} \quad (3)$$

The fluorescence anisotropy decay kinetics was given by Eq. 4,

$$r(t) = \sum \beta_i \exp\left(\frac{-t}{\phi_i}\right) \quad (4)$$

where, ϕ_i is rotational correlation time of i-th component and β_i is the corresponding amplitude. The fluorescence anisotropy decay was determined by the simultaneous global analysis of $I_{vv}(t)$ and $I_{vh}(t)$ using the Eqs 1–4. Their adequacies were confirmed by SVR and sigma value for the parallel and perpendicular, respectively. Every fluorescence measurement was performed at 25°C.

Fluorescence Quenching by Acrylamide—The fluorescence quenching experiments were based on usual Stern–Volmer equation, $F_0/F = 1 + K_{sv}[Q]$, where F_0 and F were the fluorescence intensities in the absence and presence of the quencher molecule and K_{sv} and [Q] were Stern–Volmer constant and the concentration of the quencher, respectively. The sample solution including 20 μM of α-momorcharin, which was equilibrated with various concentrations Gdn was titrated by a solution of acrylamide without changing the concentration of Gdn and protein. The fluorescence intensity was measured at the fluorescence maximum wavelength. The quenching constant K_{sv} was estimated by the slope of the Stern–Volmer plot. The collisional fluorescence quenching constant was obtained by the average fluorescence lifetime (τ_{av}) and K_{sv}.

Circular Dichroism Spectrum—Circular dichroism (CD) spectrum of α-momorcharin was recorded on a J-720 spectropolarimeter (JASCO). The sample solution of α-momorcharin was buffered with 20 mM Tris–HCl buffer, pH 7.8. The protein concentration used for CD spectrum was adjusted to 0.1 mg/ml. CD cuvettes with 1 and 5 mm of optical-path length was used for the measurements in the far- and near-UV regions, respectively.

RESULTS

The fluorescence spectra of α-momorcharin in 20 mM Tris–HCl buffer, pH 7.8 give a maximum at 328 nm. When this protein was equilibrated with 4.5 M of Gdn, the fluorescence spectrum shifted the maximum wavelength to 355 nm and the intensity was enormously reduced. These results suggest that the tryptophan

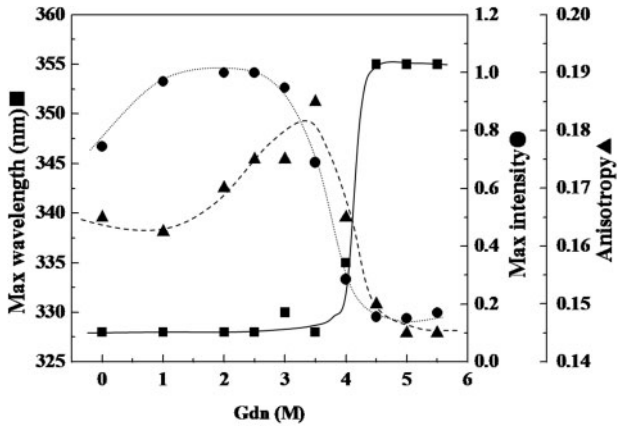

Fig. 2. **Gdn concentration dependence of fluorescence spectroscopic properties of α-momorcharin.** The concentration of the protein was 0.1 mg/ml. Filled circle, fluorescence intensity; filled triangle, steady-state fluorescence anisotropy; filled square, fluorescence maximum wavelength. Excitation wavelength was 297 nm. The fluorescence intensity and anisotropy were measured at the fluorescence maximum wavelength. The lines (dot, broken and solid) are drawn just for the aid to the eye and not based on the quantitative analysis.

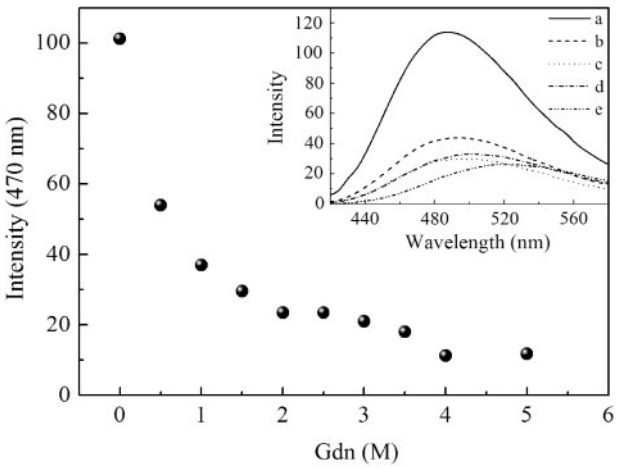

Fig. 3. **The fluorescence intensity of ANS in the solution including α-momorcharin equilibrated with various concentration of Gdn.** Inset, the fluorescence spectra of ANS versus Gdn concentration. The spectra of a, b, c, d and e are 0, 1, 2, 2.5 and 4 M Gdn, respectively. Excitation and emission wavelength were 380 and 470 nm, respectively. The concentration of α-momorcharin and ANS were 2.0 and 200 μM, respectively.

residues of α-momorcharin locate at the hydrophobic site and it is exposed to the protein surface on unfolding of the protein. The equilibratory unfolding profile monitored with the fluorescence intensity, maximum wavelength and anisotropy of α-momorcharin was shown in Fig. 2. The fluorescence maximum wavelength of α-momorcharin steeply shifted to the red side at 4 M of Gdn to reach to 355 nm at 4.5 M of Gdn. The fluorescence intensities of α-momorcharin increased once in the presence of Gdn of 0–1 M, but it decreased to 10% by the increase in Gdn concentration from 2.5 M to 4.5 M. It is more clearly shown by the steady-state fluorescence depolarization measurements that α-momorcharin would take a specific conformation state different from the native and unfolded state at the presence of 2–4 M of Gdn. This result suggests that the segmental motion of tryptophan residue of α-momorcharin would be suppressed and/or the hydration volume of momorcharin enlarged in this concentration range of Gdn.

The fluorescence of ANS is useful probe for investigating the hydrophobic pocket in proteins, since it gives the higher fluorescence intensity in the non-polar circumstance. Using this spectroscopic property, ANS has been used for the identification of the partially unfolded state (*17*). The binding of ANS with α-momorcharin equilibrated with various concentrations of Gdn were examined through the fluorescence spectrum changes (Fig. 3). The fluorescence intensity of ANS, at first sight, looks like to decrease monotonously with increase in the Gdn concentration. However, the decreasing curve of fluorescence intensity of ANS was consisted of two phases. The first phase reached once to a constant value at 2–3 M of Gdn. The fluorescence intensity decreased furthermore in increasing Gdn concentration higher than 4 M. The fluorescence maximum wavelengths of ANS shifted to the longer wavelength side with the increase in the concentration of Gdn. These results demonstrate that the

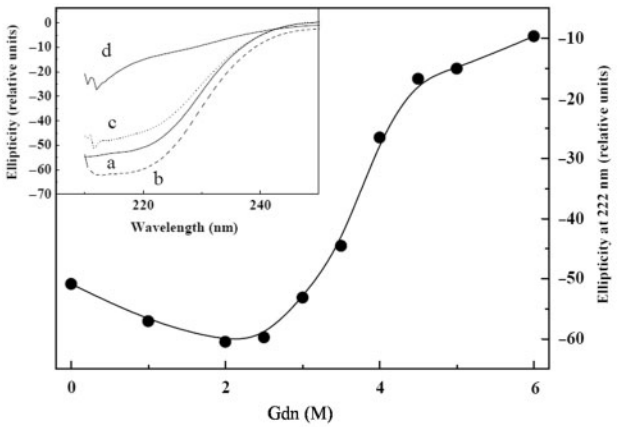

Fig. 4. **The Gdn concentration dependence of ellipticity of α-momorcharin at 222 nm.** Inset, CD spectra of α-momorcharin in the buffer solution including 0 M (a), 2 M (b), 3 M (c), 4 M (d) and 5 M (e) of Gdn. The concentration of α-momorcharin was 0.1 mg/ml.

hydrophobic parts of α-momorcharin would be concealed at 2–3 M of Gdn.

Figure 4 shows the effects of Gdn on the CD spectrum of α-momorcharin. The ellipticity at 222 nm was increased as increasing in the Gdn concentration at 0–2.5 M. But, it contrarily decreased at higher than 3 M of Gdn. At the concentration higher than 5 M of Gdn, very small ellipticity was recognized at the wavelength 217 nm. When the ellipticity at 222 nm which was the indicator for the significant presence of α-helix was plotted against Gdn concentration, the maximum value was found at 2.5 M Gdn solution. In order to estimate precisely the composition of secondary structure of protein, the spectrum has to be measured in the wide range of wavelength. Unfortunately, the optical absorption of

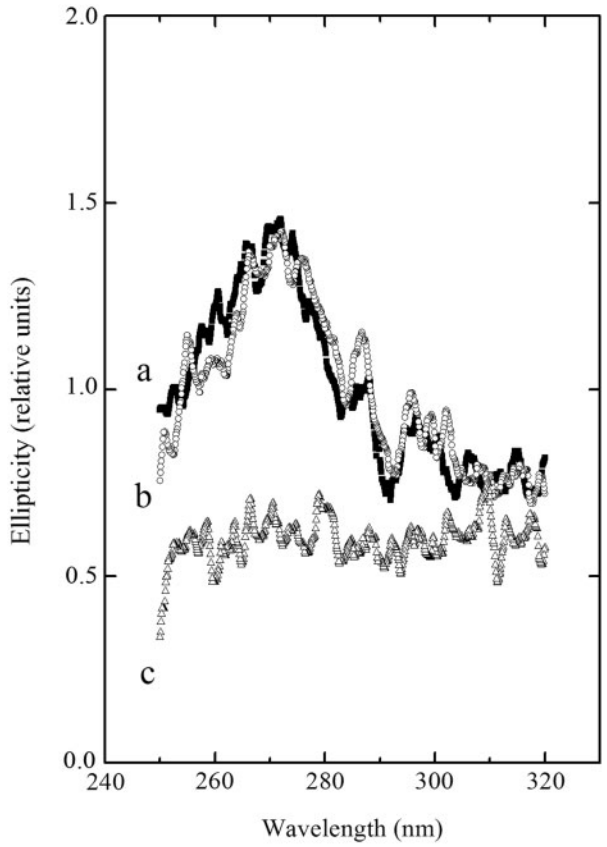

Fig. 5. **The CD spectra of α-momorcharin in the near-UV region.** The spectra of a, b and c are observed at 0, 3 and 5 M Gdn, respectively.

Table 1. **Fluorescence quenching parameters of α-momorcharin by acrylamide.**

Concentration of Gdn (M)	K_{SV} (M^{-1})	τ_{av} (ns)	k_q ($M^{-1}s^{-1}$)
0	4.7	2.90	1.62
2	2.3	3.43	0.67
3	2.6	3.42	0.76
5	4.8	1.48	3.24

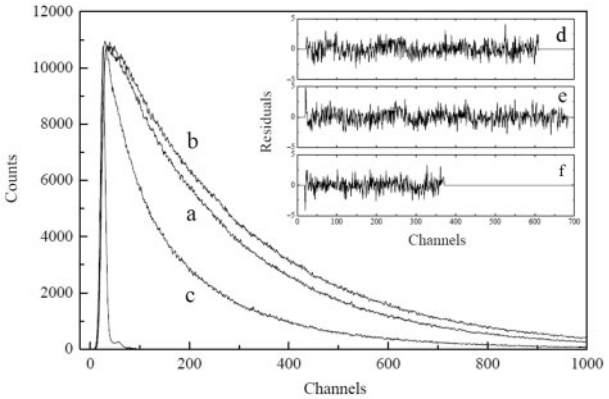

Fig. 6. **The fluorescence decay curves(a, b and c) of α-momorcharin in the buffer solution including 0 M (a), 3 M (b) and 5 M (c) excited at 297 nm.** The residual plots giving the best fit are given by d, e and f. Spike-like curves indicate the response function for the excitation pulse. Channel width was 11 ps/ch. The emission wavelength were 330 nm (a, b) and 350 nm (c), respectively. The concentration of α-momorcharin was 0.08 mg/ml.

the high concentration of Gdn disturbs and distorts the CD spectrum of α-momorcharin at the far-UV region. Therefore, it is difficult to estimate precisely the content of α-helix of α-momorcharin equilibrated with 2.5 M of Gdn solution. However, it should be noted that the ellipticity at 222 nm was distinctly increased in the presence of 2.5 M Gdn.

CD spectrum of α-momorcharin was measured at near-UV region to examine the Gdn effects on the tertiary structure in various concentrations. As shown in Fig. 5, the pronounced positive ellipticity was found at the absorption wavelength region of aromatic amino acid (260–300 nm) in the buffer solutions including 0 and 3 M Gdn, while they were not recognized in 5 M of Gdn solution. The broad band intensity seen at 260–280 nm in the absence of Gdn was almost same as one in the 3 M Gdn solution. But is should be noted that the positive cotton effect seen at 289 nm was more remarkable in the presence of 3 M Gdn than that in the absence of Gdn, although it is hard to discuss quantitatively since the S/N ratio was low. These results demonstrate the tertiary structure of α-momorcharin is retained, or rather increased at the presence of 3 M Gdn.

Fluorescence dynamic quenching experiments were performed to investigate the conformational change around the tryptophan residue. The Stern–Volmer plots of α-momorcharin in the solutions including 0, 2, 3 and 5 M of Gdn were so linear that Stern–Volmer constant could be estimated precisely (data not shown). The apparent quenching constant, K_{sv} of the native state was larger than that of the unfolded. But the accessibility of the quencher to the tryptophan residue must be evaluated by the collisional quenching constant, k_q, because the cross section of the quenching depends on the fluorescence lifetime. According to the fluorescence quenching theory, the relation between K_{sv} and k_q is given by $K_{sv} = k_q \times \tau_{av}$. The resulting quenching parameters are summarized in Table 1. The lower accessibility of the quencher molecule to the tryptophan residue was found in the solution equilibrated with 2 M of Gdn. It should be noted that the collisional quenching constant of the native α-momorcharin is 2.5-fold larger than that of α-momorcharin in 2 M of Gdn.

The steady-state fluorescence and CD spectroscopic studies suggested that α-momorcharin reached to the specific conformation state in the presence of around 2.5 M Gdn between the native and unfolded states. In order to characterize the features in conformation and dynamics of this state, the time-resolved fluorescence studies were examined. For the measurement of time-resolved fluorescence study, α-momorcharin was excited at 297 or 285 nm. On the excitation at 297 nm, Trp residue is excited exclusively in momorcharin and both of Trp and Tyr are excited by 285 nm pulse. Figures 6 and 7 show the fluorescence decay curves of α-momorcharin equilibrated with 0, 3 and 5 M of Gdn. Their decay parameters giving the best fit to the sum of exponential

function were summarized in Table 2. The fluorescence decay profiles excited at 285 nm exhibited more truncated form than that excited at 297 nm in the presence of 0 and 3 M of Gdn to suggest that they would include negative pre-exponential factor in the decay kinetics. In the presence of 5 M Gdn, the decay profiles of the momorcharin were independent on the excitation wavelength and their decay kinetics was described with the sum of triple exponentials.

The detail analysis by non-linear curve fitting demonstrated that the fluorescence state of α-momorcharin was stabilized in the presence of 3 M of Gdn. Clearly shown in Table 2, the fluorescence of momorcharin excited not at 297 nm but 285 nm included negative pre-exponential factors in their decay kinetics in the absence and the presence of 3 M of Gdn. Such excitation wavelength dependences of the fluorescence decay kinetics suggest that the excitation energy transfer from tyrosine to tryptophan residue would involve in the energy relaxation process of tryptophan. The results given in Table 2 also demonstrate that the fluorescence decay time of donor corresponding to the negative pre-exponential factor in the solution of 3 M of Gdn is faster than that in the absence of Gdn. Based on the simple kinetic analysis, the fluorescence decay of the energy acceptor (tryptophan) is given by Eq. 5, where A_0 and D_0 are constant relating with the initially populated acceptor and donor molecules, τ_D and τ_A are the fluorescence decay times of energy donor and acceptor, respectively and k_t is the energy transfer rate (*18*).

$$f(t) = \left[\frac{k_t D_0}{(1/\tau_A) - (1/\tau_D)}\right]\left[\exp\left(\frac{-t}{\tau_D}\right) - \exp\left(\frac{-t}{\tau_A}\right)\right] + A_0 \exp\left(\frac{-t}{\tau_A}\right) \quad (5)$$

When tyrosine residues have shorter fluorescence lifetime than tryptophan in Eq. 5, the energy transfer rate can be estimated using the decay rate corresponding to the negative pre-exponential factor through Eq. 6.

$$\frac{1}{\tau_D} = k_t + \frac{1}{\tau_0} \quad (6)$$

When 3.27 ns was used as the fluorescence lifetime of the tyrosine residue in the absence of the energy acceptor (*19*), the energy transfer rates were calculated to be 0.55/ns and 1.58/ns in the absence and presence of 3 M Gdn, respectively.

The time-resolved fluorescence depolarization studies provide the information on the segmental motion of Trp residue in the polypeptide cage of protein. The fluorescence anisotropy decay curves of α-momorcharin equilibrated with 0, 3 and 5 M of Gdn were shown in Fig. 8. They were described with the double exponential kinetics. One of two rotational correlation times is short and the other is longer. The longer correlation time (ϕ_2) of the native state was 30.8 ns and it was slightly shorter than that in the 3 M of Gdn solution. These two rotational correlation times were consistent with the values calculated using the Einstein–Stokes relation and assuming the specific volume is 0.75 ml/mg and hydration is 0.4. Therefore, the slower rotational correlation time observed here must be attributed to one of the entire rotation of α-momorcharin. The results given in Table 3 suggest the hydration volume of α-momorcharin would be larger in 3 M of Gdn solution. The longer correlation time (ϕ_2) of α-momorcharin equilibrated with 5 M of Gdn was rather shorter. Probably, it would be caused by the unfolding of the protein and the correlation time would be attributed to the rotational motion of the resulting larger peptide elements including the Trp residue. Since the intrinsic anisotropy (r_0) was 0.30 in every case,

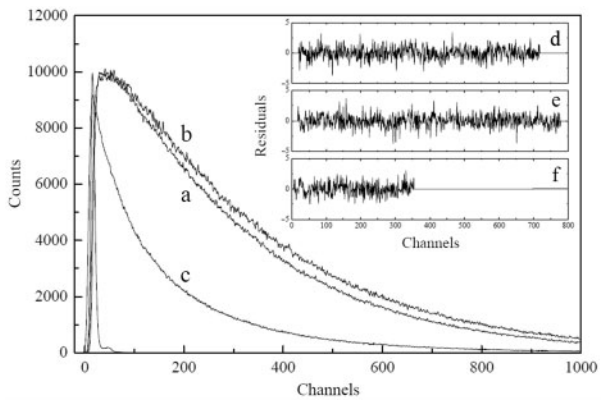

Fig. 7. **The fluorescence decay curves(a, b and c) of α-momorcharin in the buffer solution including 0 M (a), 3 M (b) and 5 M (c) excited at 285 nm.** The residual plots giving the best fit are given by d, e and f. Spike-like curves indicate the response function for the excitation pulse. Channel width was 11 ps/ch. The emission wavelength were 330 nm (a, b) and 350 nm (c), respectively. The concentration of α-momorcharin was 0.08 mg/ml.

Table 2. **The fluorescence decay parameters of α-momorcharin.**

Excitation	Gdn conc.	α_1	α_2	α_3	τ_1(ns)	τ_2(ns)	τ_3(ns)	σ	SVR
297 nm	0 M[a]	0.93	0.07	–	3.07	0.57	–	1.09	1.80
	2 M[a]	0.97	0.03	–	3.51	0.65	–	1.12	1.81
	3 M[a]	0.97	0.03	–	3.52	0.63	–	1.10	1.71
	5 M[b]	0.46	0.37	0.17	2.56	0.72	0.18	1.04	1.97
285 nm									
	0 M[a]	1.24	−0.24	–	3.52	1.16	–	1.03	1.89
	2 M[a]	1.22	−0.22	–	4.21	0.55	–	1.05	1.90
	3 M[a]	1.21	−0.21	–	4.26	0.53	–	1.06	1.89
	5 M[b]	0.40	0.42	0.18	2.73	0.90	0.20	1.05	2.03

Excitation wavelength. [a]Emission wavelength, 330 nm. [b]Emission wavelength, 350 nm. The fluorescence decay kinetics was given as the linear combination of exponentials, $F(t) = \sum \alpha_i \exp(-t/\tau_i)$.

the motional freedom (f) of Trp residue in the peptide cage of α-momorcharin is estimated by the relation, $f = \beta_1/(\beta_1 + \beta_2)$. The results on the motional freedom given in Table 3 suggest that the segmental motion of Trp would be remarkably suppressed by the conformational change in the solution of 3 M of Gdn.

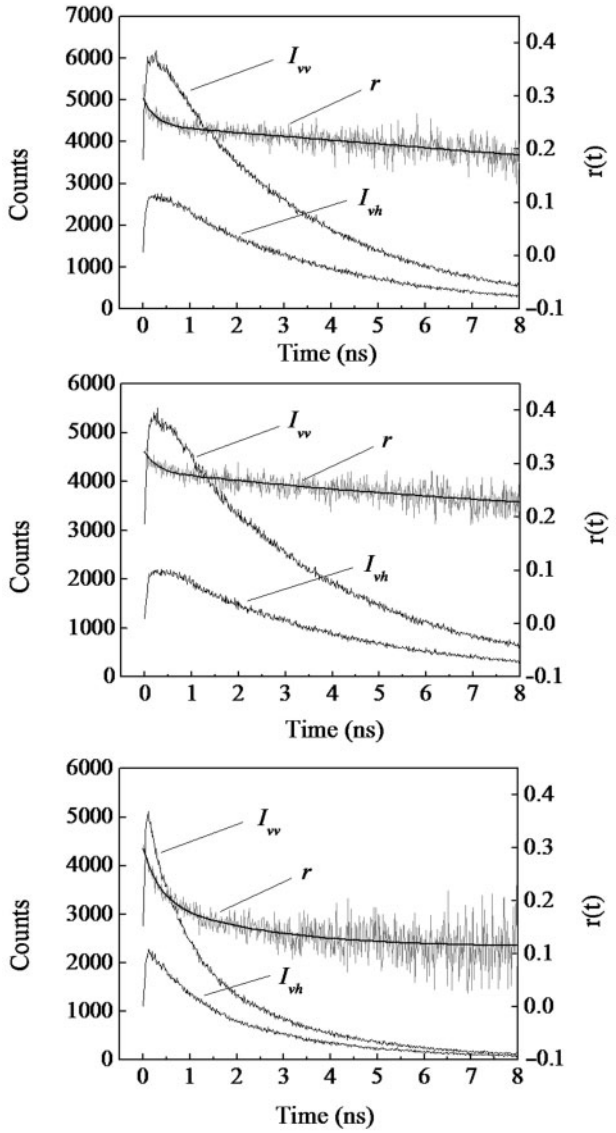

Fig. 8. **The fluorescence anisotropy decay of α-momorcharin in the solution including 0 M (a), 3 M (b) and 5 M (c).** The excitation wavelength was 297 nm and the fluorescence was measured at 330 nm for 0 and 3 M and 350 nm for 5 M Gdn. The decays of vertical and horizontal components used for the determination of the anisotropy decay parameters were indicated by I_{vv} and I_{vh}, respectively. The fluorescence anisotropy decay curves (r) were obtained by the equation, $r(t) = (I_{vv}(t) - GI_{vh}(t))/(I_{vv}(t) + 2GI_{vh}(t))$. ($G = 1.2$).

DISCUSSION

The fluorescence and CD spectroscopic studies consistently demonstrated that α-momorcharin reached to the unfolded state through a peculiar intermediate state by being equilibrated with a chemical denaturant, Gdn similarly with β-momorcharin. But the present results also demonstrated that the unfolding intermediate state of α- and β-momorcharin retained the own characteristics, regardless of their similar X-ray crystallographic structures and amino acid sequences. The unfolding intermediate state of β-momorcharins formed in the presence of 2–3 M of Gdn showed similar properties to the well-known MG state of other protein (*3*). The secondary structure was almost retained and some hydrophobic sites were exposed to the protein surface to allow the access of ANS. On the other hand, α-momorcharin formed unique intermediate state. On the transition from the native state to the intermediate state, the tertiary structure were retained as shown in CD spectra at near-UV region, and the bound ANS molecules were excluded from the hydrophobic pocket of α-momorcharin resulting in a decrease in the fluorescence intensity of ANS. At the same time, the contents of secondary structure, probably α-helix, of α-momorcharin was increased at the intermediate state.

The peculiarity of the unfolding intermediate state of α-momorcharin was especially recognized in the conformation and dynamics of Trp192 near the active site. The involvement of energy transfer process from Tyr to Trp was observed in the native and intermediate states and not in the unfolded state of the momorcharin. The energy transfer rates experimentally decided based on the fluorescence decay kinetics of the energy acceptor, Trp192 suggest that the distance between Trp and the nearest neighbouring tyrosine residue would shrink on the transition from the native to the intermediate state because the energy transfer rate of α-momorcharin increased from 0.55/ns to 1.58/ns. According to Förster's fluorescence resonance excitation energy transfer (FRET) formalism, the distance (R) between tryptophan and tyrosine is estimated by the energy transfer efficiency (E), which is given by the experimentally determined τ_D through Eq. 7. The critical distance (R_0) defined as the energy transfer distance where the energy transfer rate (k_t) is just same as fluorescence decay rate of the energy donor.

$$\frac{1}{E} - 1 = \left(\frac{R}{R_0}\right)^6 \tag{7}$$

Eisinger *et al.* (*20*) showed the critical distance for the energy transfer between tyrosine and tryptophan

Table 3. **The fluorescence anisotropy decay parameters of α-momorcharin.**

	β_1	β_2	ϕ_1 (ps)	ϕ_2 (ns)	σ	SVR (I_{vv})	SVR (I_{vh})	f	θ (deg)
0 M Gdn[a]	0.05	0.25	280	30.8	1.03	1.91	2.07	0.17	20.0
2 M Gdn[a]	0.02	0.28	560	32.2	1.05	1.89	1.92	0.07	12.6
3 M Gdn[a]	0.02	0.27	580	34.5	1.07	1.81	1.96	0.07	12.6
5 M Gdn[b]	0.12	0.18	390	11.4	0.99	2.06	1.92	–	–

Excitation wavelength, 297 nm. [a]Emission wavelength, 330 nm. [b]Emission wavelength, 350 nm.

was 13 Å. When this value was applied for the present case of α-momorcharin, the distances between Trp192 and the nearest Tyr residue were estimated to be 11.8 and 9.9 Å for the native and the intermediate state of α-momorcharin, respectively. According to the X-ray crystallographic structure of α-momorcharin, the nearest neighbouring tyrosine residue, Tyr70 of α-momorcharin locates 8.23 Å apart from Trp192. This distance may be a little shorter than the energy transfer distance obtained here for the native momorcharin. But, this discrepancy would not be unreasonable, because the experimentally decided energy transfer distance correspond to one between the absorption and fluorescence transition moments of Tyr and Trp. Assuming that Tyr70 of α-momorcharin contributes as the excitation energy donor, the distance between tryptophan and tyrosine of α-momorcharin would shrink about 2 Å at the intermediate states. The approach of Trp192 to Tyr70 is one of the specific conformational changes induced in the intermediate state of α-momorcharin.

The unique conformations at the active site of momorcharins in the unfolding intermediate state were also confirmed in results of the time-resolved fluorescence depolarization studies. The fluorescence anisotropy decay of α-momorcharins in the intermediate state was described with double exponential kinetics. Equation 4 can be rearranged to Eq. 8 to extract the features of dynamic properties of segmental motions of Trp, assuming that the rotational motions of tryptophan residue and the whole protein are independent each other.

$$r(t) = r_0\left\{f\exp\left(-\frac{t}{\phi_f}\right) + (1-f)\right\}\exp\left(-\frac{t}{\phi_p}\right) \qquad (8)$$

The rotational correlation time of peptide element including tryptophan residue (ϕ_f) and the entire rotational correlation time (ϕ_p) are connected with the experimentally decided ϕ_1 and ϕ_2. The motional freedom of peptide element of Trp, f, is given as the fractioned β_1 and is represented by the semi-cone angle (θ) based on the following relation (*21–23*).

$$(1-f)^{1/2} = \frac{1}{2}\cos\theta(\cos\theta + 1) \qquad (9)$$

The segmental motion of Trp192 of α-momorcharin in the native state retained fairly large motional freedom and the correlation time is shorter at the vicinity of active site. At the unfolding intermediate state, the dynamical parameters of Trp192 were drastically changed. The segmental motion of Trp192 of α-momorcharin was remarkably suppressed as revealed by the reducing of motional freedom and prolonged correlation time suggesting that the peptide element including Trp192 would be packed more compactly. The anticipated features in conformation and dynamics were figured out in Fig. 9 based on the results of the energy transfer and fluorescence anisotropy decay analysis obtained here. When the motional freedom was presented with the semi-cone angle, Trp192 of α-momorcharin reduced it from 20.0° to 12.6° on the transition to the unfolding intermediate state.

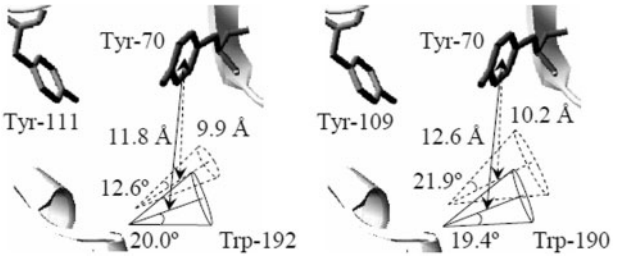

Fig. 9. **The anticipated change in the conformation and dynamics of α-momorcharin induced in the unfolding intermediate state (left).** The segmental motion of Trp192 is represented with solid (native state) and dotted (unfolding intermediate state) cone. The distance between Trp and Tyr was drawn by the line between centres of Tyr and the cone. The changes in the conformation and dynamics of β-momorcharin in the partially unfolded state are shown in the right. (*19*)

It may be useful to compare the features in conformation and dynamics of the unfolding intermediate state of α-momorcharin with those of β-momorcharin, because these two momorcharins preserve the higher homologies of amino acid sequence and tertiary structure each other. The unfolding intermediate state of β-momorcharin presumably correspond to the partially unfolded state generally known as MG state, since its hydrophobic site was exposed to the surface, Trp190 mobilized and the hydration volume enlarged. On the other hand, the intermediate state of α-momorcharin showed some peculiar conformational and dynamic properties. The hydrophobic site being accessible of ANS was rather sealed and the internal motion of Trp192 was rather suppressed. These properties are inconsistent with the general concepts of MG state. The structure of the native protein is stabilized by many physical forces with different natures. Hydrogen bonds determine the formation of secondary structure and hydrophobic interactions are responsible for the compaction, whereas electrostatic and van der Waals interactions stabilize the unique tertiary structure. Because of their different nature responding to the changes in the protein environments, some environments might turn off one conformational factor, whereas the efficiency of other force will not change or even will be enhanced under the same conditions. Based on such consideration, it is reasonable to consider that the folding/unfolding intermediate state would have various characteristics according to the amino acid sequences and native structure. Hitherto, the restricted state of tryptophan motion (N') and pre-MG state have been reported in addition to the MG state between the native and unfolded state (*24*). The unfolding intermediate state of α-momorcharin exhibited very similar property with the Trp-restricted state, N', reported on other protein because Trp192 certainly suppressed its own segmental motion and approached to the hydrophobic core side in the intermediate state.

Although the X-ray crystallographic structures of two momorcharins are very similar, α-momorcharin is composed of more α-helix and β-sheet and, furthermore,

the packing density around Trp residue is higher than β-momorcharin as shown in Fig. 9. It is now difficult to specify the mechanism to form the quite different unfolding intermediate states of two momorcharins. But, the participation of the second structure propensity would be reasonably speculated because it is known that interaction between α-helices is important factor to stabilize the partially unfolded state on unfolding/folding process of protein (*25*). The increase in the α-helix content of protein has been reported on the transition from the native to the intermediate state. Watanabe *et al*. (*26*) showed that some sites of β-sheet converted to α-helix in the partially unfolded state of some proteins. The content of secondary structure, not necessarily specified to α-helix by the distortion of the CD spectrum by the presence of high concentration of Gdn, increased 20% in the intermediate of α-momorcharin. The interaction between the α-helices would produce the change in the packing structure of α-momorcharin to restrict the motion of tryptophan residue near the active site. Also, the resulting stabilization of the intermediate state is consistent with experimental results that α-momorcharin unfolded at the higher concentration of Gdn than β-momorcharin of which content of secondary structure was decreased a little at the intermediate state.

The studies on the protein folding/unfolding do not only provide essential information on the mechanism by which the tertiary structure of protein is constructed but also are inevitable to clarify the protein trafficking mechanism in living cell (*27*). In the present study, the tertiary structures of α-momorcharin would be constructed through the intermediate state quite different with one of β-momorcharin. The intermediate state of β-momorcharin exposed hydrophobic sites to the protein surface and, on the other hand, α-momorcharin preserves the native like structure to conceal the hydrophobic site to suppress the movement of the constituting peptide elements. Although two momorcharins exhibit the similar enzymatic activity *in vitro* (data is not shown), they may be distributed to different parts in living cell during the folding process. The former may be distributed to the hydrophobic parts in the cell including membranes and the latter locate at the hydrophilic parts. The interactions of the unfolding intermediate state of momorcharins with membrane system are under investigation.

REFERENCES

1. Ren, J., Wang, Y., Dong, Y., and Stuart, I.D. (1994) The *N*-glycosidase mechanism of ribosome-inactivating proteins implied by crystal structures of α-momorcharin. *Structure* **2**, 7–16
2. Lakowicz, J.R. (1999) *Principles of Fluorescence Spectroscopy* 2nd edn, Kluwer Academic/Plenum Publishers., New York
3. Fukunaga, Y., Nishimoto, E., Yamashita, K., Otosu, T., and Yamashita, S. (2007) The partially unfolded state of β-momorcharin characterized with steady-state and time-resolved fluorescence studies. *J. Biochem.* **141**, 9–18
4. Kuwajima, K. (1989) The molten globule state as a clue for understanding the folding and cooperativity of globular-protein structure. *Proteins* **6**, 87–103
5. Radford, S.E., Dobson, C.M., and Evans, P.A. (1992) The folding of hen lysozyme involves partially structured intermediates and multiple pathways. *Nature* **358**, 302–307
6. Ptitsyn, O.B. (1995) Molten globule and protein folding. *Adv. Protein. Chem.* **47**, 83–229
7. Arai, M. and Kuwajima, K. (2000) Role of the molten globule state in protein folding. *Adv. Protein. Chem.* **53**, 209–282
8. Koshiba, T., Yao, M., Kobashigawa, Y., Demura, M., Nakagawa, A., Tanaka, I., Kuwajima, K., and Nitta, K. (2000) Structure and thermodynamics of the extraordinarily stable molten globule state of canine milk lysozyme. *Biochemistry* **39**, 3248–3257
9. Samuel, D., Kumar, T.K.S., Srimathi, T., Hsieh, H., and Yu, C. (2000) Identification and characterization of an equilibrium intermediate in the unfolding pathway of an all β-barrel protein. *J. Biol. Chem.* **275**, 34968–34975
10. Nitta, K. (2002) Alpha-lactalbumin and (calcium-binding) lysozyme. *Methods Mol. Biol.* **172**, 211–224
11. Schulman, B.A., Kim, P.S., Dobson, C.M., and Redfield, C. (1997) A residue-specific NMR view of the non-cooperative unfolding of a molten globule. *Nat. Struct. Biol.* **4**, 630–634
12. Anfinsen, C.B., Haber, E., Sela, M., and White, F.H. (1961) The kinetics of formation of native ribonuclease during oxidation of the reduced polypeptide chain. *Proc. Natl Acad. Sci.* **47**, 1309–1314
13. Anfinsen, C.B. (1973) Principles that govern the folding of protein chains. *Science* **181**, 223–230
14. Kobashigawa, Y., Demura, M., Koshiba, T., Kumaki, Y., Kuwajima, K., and Nitta, K. (2000) Hydrogen exchange study of canine milk lysozyme: stabilization mechanism of the molten globule. *Proteins* **40**, 579–589
15. Fong, W.P., Poon, Y.T., Wong, T.M., Mock, J.W.Y., Ng, T.B., Wong, R.N.S., Yao, Q.Z., and Yeung, H.W. (1996) A highly efficient procedure for purifying the ribosome-inactivating proteins α- and β-momorcharins from *Momordica charantia* seeds. N-terminal sequence comparison and establishment of their *N*-glycosidase activity. *Life Sci.* **59**, 901–909
16. McKinnon, A.E., Szabo, A.G., and Miller, D.R. (1977) The deconvolution of photoluminescence data. *J. Phys. Chem.* **81**, 1564–1570
17. Uversky, V.N., Winter, S., and Löber, G. (1996) Use of fluorescence decay times of 8-ANS-protein complexes to study the conformational transitions in proteins which unfold through the molten globule state. *Biophys. Chem.* **60**, 79–88
18. Oishi, O., Yamashita, S., Nishimoto, E., Lee, S., Sugihara, G., and Ohno, M. (1997) Conformations and orientations of aromatic amino acid residues of tachyplesin I in phospholipid membranes. *Biochemistry* **36**, 4352–4359
19. Ross, J.B.A., Laws, W.R., Rousslong, K.W., and Wyssbrod, H.R. (1992) Tyrosine fluorescence and phosphorescence from proteins and polypeptide. in *Topics in Fluorescence spectroscopy* (Lakowicz, J.R., ed.) Vol. 3, pp. 1–63, Biochemical Applications, Plenum Press, New York
20. Eisinger, J., Feuer, B., and Lamola, A.A. (1969) Intramolecular singlet excitation transfer. Applications to polypeptides. *Biochemistry* **8**, 3908–3915
21. Lipari, G. and Szabo, A. (1982) Model-free approach to the interpretation of nuclear magnetic resonance relaxation in macromolecules. 2. Analysis of experimental results. *J. Am. Chem. Soc.* **104**, 4559–4570
22. Chen, R.F., Knutson, J.R., Ziffer, H., and Porter, D. (1991) Fluorescence of tryptophan dipeptides: correlations with the rotamer model. *Biochemistry* **30**, 5184–5195
23. Nishimoto, E., Yamashita, S., Szabo, A.G., and Imoto, T. (1998) Internal motion of lysozyme studied by time-resolved

fluorescence depolarization of tryptophan residues. *Biochemistry* **37**, 5599–5607
24. Kuznetsova, I.M., Stepanenko, O.V., Turoverov, K.K., Zhu, L., Zhou, J.-M., Fink, A.L., and Uversky, V.N. (2002) Unraveling multistate unfolding of rabbit muscle creatine kinase. *Biochim. Biophys. Acta* **1596**, 138–155
25. Koshiba, T., Yao, M., Kobashigawa, Y., Demura, M., Nakagawa, A., Tanaka, I., Kuwajima, K., and Nitta, K. (2000) Structure and thermodynamics of the extraordinarily stable molten globule state of canine milk lysozyme. *Biochemistry* **39**, 3248–3257
26. Watanabe, M., Kobashigawa, Y., Aizawa, T., Demura, M., and Nitta, K. (2004) A non-native α-helix is formed in the β-sheet region of the molten globule state of canine milk lysozyme. *Protein. J.* **23**, 335–342
27. Dobson, C.M. (2003) Protein folding and misfolding. *Nature* **426**, 884–890